

# INVESTIGATION OF THE MÖBIUS ACCELERATOR AT CESR \*

S. Henderson<sup>†</sup>, M. Billing, R. Holtzapple, R. Littauer, B. McDaniel, D. Rice, D. Rubin, D. Sagan, R. Talman, and A. Temnykh, Cornell University, Ithaca, NY

## Abstract

We present a status report on the investigation of the Möbius scheme for producing equal-emittance round beams at CESR [1]. An insert has been constructed with six 45° rotated quadrupoles which interchange horizontal and vertical betatron oscillations on each passage. We describe the single-beam dynamics and the limitations introduced by the chromaticity correcting sextupoles. We also report on our two-beam experience.

## 1 INTRODUCTION

The collision of round beams (rather than flat) shows promise for substantial increases in luminosity at colliding beam facilities. We reported previously [2] on an experimental investigation of round-beam  $e^+e^-$  collisions at the Cornell Electron Storage Ring (CESR), in which beam-beam tunes parameters,  $\xi$ , as large as 0.09 were achieved. In that study, the beams were made round at the interaction point (IP) by resonant coupling in a lattice having equal betatron functions at the IP ( $\beta_x^* = \beta_y^*$ ). Transverse emittances were made equal by tuning the lattice to the coupling resonance ( $Q_x - Q_y = \text{integer}$ ) and powering weak skew quadrupoles. Since we were unable to produce competitive luminosity due to limitations of the existing IR quadrupoles (only rather large values of  $\beta^*$  were accessible), our studies focused on the beam-beam tunes shift  $\xi$  instead. Indeed, those results confirmed the expectation [3] of improved beam-beam performance from round-beam collisions.

The Möbius scheme, proposed by Talman, provides an alternative, potentially superior, way to obtain full emittance coupling [1]. A lattice insert is constructed which exchanges the horizontal and vertical betatron oscillations. When such an insert is added to an ordinary uncoupled accelerator lattice, horizontal betatron motion on one turn becomes vertical on the next turn and vice versa. It has been our hope that the Möbius scheme would provide a more robust method of producing round-beams, avoiding the operational difficulties that are associated with resonant coupling. We present a status report on our investigation of the Möbius scheme at CESR.

## 2 MÖBIUS LATTICE DESIGN

### 2.1 General Properties

An insert with the desired  $x - y$  exchange property can be constructed by axially rotating a special bend-free sec-

tion of the lattice through 45°. If the insert has  $\alpha_x = \alpha_y$ ,  $\beta_x = \beta_y$  at the boundaries, and betatron phase advances that differ by  $\pi$ , then its  $4 \times 4$  transport matrices before and after rotation will be

$$M_{erect} = \begin{pmatrix} T & 0 \\ 0 & -T \end{pmatrix} \quad (1)$$

and

$$M_{skew} = \begin{pmatrix} 0 & T \\ T & 0 \end{pmatrix} \quad (2)$$

where  $T$  is a  $2 \times 2$  transport matrix. We will refer to the lattices before and after rotation of the Möbius insert as the *erect* and *Möbius* lattices, respectively.

The normal mode tunes of the Möbius lattice are denoted  $Q_{1,-1}$  and are related to the erect-lattice tunes by

$$Q_1 = \frac{1}{2}(Q_x + Q_y) - \frac{1}{4}, \quad Q_{-1} = \frac{1}{2}(Q_x + Q_y) + \frac{1}{4} \quad (3)$$

Since the tunes are always separated by  $\frac{1}{2}$ , we have only one adjustable parameter for making tune adjustments. However, the separate values of  $Q_x$  and  $Q_y$  may affect lattice properties such as resonances (see below).

### 2.2 Möbius Insert Design

We have constructed a Möbius insert from existing CESR quadrupoles which are rotated by 45°. The insert includes 6 quadrupoles in the North IR straight straddling the symmetry point opposite the south IR (the collision point) where the CLEO detector is located. The machine layout and one example of insert optics are shown in Figure 1. The insert is taken to extend between the centers of vertical separators (VSW,VSE) on either side of the North IP. As described above, the insert satisfies the Möbius requirements of  $\beta_x = \beta_y$  and  $\alpha_x = \alpha_y$  at the boundaries and  $\phi_x = \phi_y + \pi$  through the insert. The optics design maintained the existing position of all the CESR quadrupoles but required the installation of two additional quadrupoles which are not in use in ordinary CESR operation. Polarity reversal (relative to ordinary CESR operation) of one quadrupole on either side of the insert was required to properly match the insert optics to the CESR arcs.

The six quadrupoles which form the insert are mounted on individual rotators which allow manual rotation from erect to 45°. Precision angle adjustment is provided at the 0° and 45° positions. Upon rotation the quadrupole centers remain fixed to within 0.25 mm.

### 2.3 Möbius Lattice

Three Möbius lattices have been studied thus far, one of which is shown in Figure 2. Apart from the Möbius insert

\* Work supported by the National Science Foundation.

† Email: sdh9@cornell.edu

### 3 EXPERIMENTAL

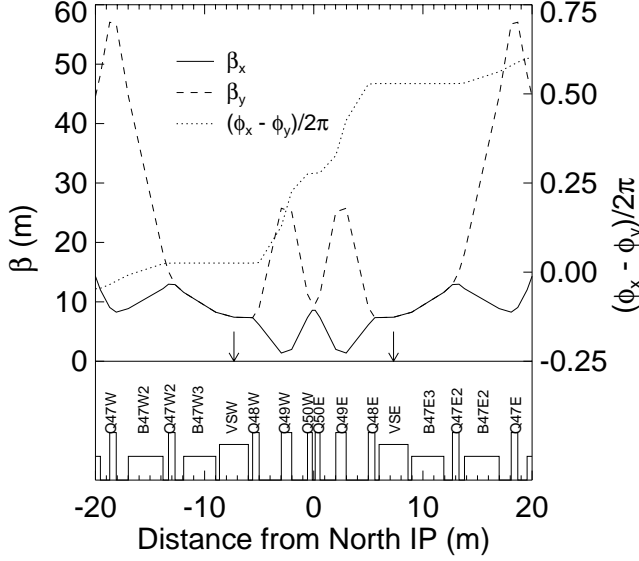


Figure 1: Möbius insert layout and optics. Quadrupoles (Q), bends (B) and vertical separators (V) are shown. Arrows mark the insert boundaries.

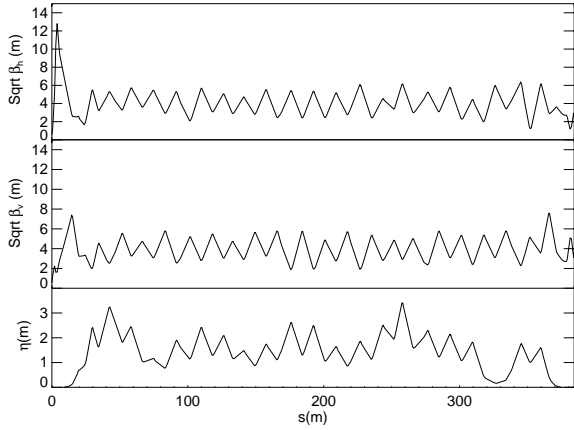


Figure 2: Möbius lattice functions for one-half of the CESR ring. The collision point (the South IR) is at the left and the Möbius insert (the North IR) is at the right.

properties described above, the lattice has the following additional features. The dispersion vanishes in both the north and south interaction regions. The high- $\eta$  point in the ring ( $\sim 260$  m) is located at the injection point to take advantage of off-energy injection into CESR, a feature which improves injection efficiency and reduces losses at the peak- $\beta_x$  point in the IR. The IR optics match those of the round-beam collision studies ( $\beta_x^* = \beta_y^* = 30$  cm,  $\eta^* = 0$ ). Three lattices (hereafter referred to as A,B,C) have been studied thus far. All have the features described above, but differ primarily in their operating points (Möbius tunes  $Q_1 = 9.82$  (A), 10.32 (B) and 9.89 (C)).

Generally, machine studies shifts began with the erect lattice. After recovery of injection conditions, the tunes were corrected and the closed orbit flattened by standard methods. The Möbius insert quadrupoles were then rotated and injection conditions recovered. Since the rotated quadrupole centers do not remain perfectly fixed, further orbit correction was required. This was accomplished with a merit-function minimization technique which took into account the closed-orbit response in both transverse planes to a single corrector. Typically, the corrected closed orbit had  $x_{rms}, y_{rms} < 1$  mm.

The initial lattice optics correction was performed in the erect lattice. Normal-mode betatron phase advance measurements in the Möbius lattice agreed with theoretical expectations.

### 4 RESULTS AND DISCUSSION

#### 4.1 Single Beam Dynamics

We observed early in our investigation that a beam could be stored in the Möbius lattice rather easily, but that the tune plane was broken into narrow bands by resonances. The thrust of our efforts to date has been to understand the single-beam dynamics of the Möbius accelerator.

Tune scans were performed in the various lattices to determine the operating range in the tune plane. Figure 3 shows a tune scan of lattice B, together with the results of a tracking program. The experimental data are shown as dark bands and represent the regions in  $Q_1$  in which a beam could be stored with long lifetime ( $\tau > 90$  min). The tracking results show the maximum horizontal amplitude reached in 1000 turns for a particle launched at the IP with displacements  $5\sigma_E$  and  $5\sigma_x$  (the normal modes at the IP lie along  $45^\circ$  diagonals so that  $x$  displacement excites both normal modes). Regions with good lifetime correspond rather well to those predicted from the tracking results.

The tune plane is dominated by rather strong betatron and synchrobetatron resonances. Betatron resonances which are excited by field errors are as follows: dipole errors,  $1/2n, n$ ; quadrupoles errors,  $1/4n, 1/2n, 3/4n, n$ ; and sextupole errors,  $1/6n, 1/3n, 1/2n, 2/3n, 5/6n, n$  where  $n$  is an integer. The “extra” lines are an inherent property of a strongly coupled lattice in which the normal mode tunes are separated by  $1/2$ ; they arise from one of the normal mode tunes satisfying the usual resonance conditions, or from sum resonances such as  $Q_1 + Q_{-1} = n, Q_1 + 2Q_{-1} = n$ . In addition, synchrobetatron resonance lines are excited by dispersion in sextupoles [4]. A simple model shows that the following sidebands are excited: integer  $\pm 1/2Q_s, \pm Q_s, \pm 2Q_s$ ; half-integer  $\pm 1/2Q_s, \pm Q_s, \pm 2Q_s$ ; and quarter-integer  $\pm 1/2Q_s$ . Several of these lines are clearly seen in the tracking data shown in the Figure. Finally, a mismatch at the Möbius insert (e.g.,  $\beta_x \neq \beta_y$ ) creates regions of instability near  $Q_1 = 1/4n, 1/2n, 3/4n, n$  [1].

There are two important features to emphasize. First, the density of “structural” resonance lines is doubled relative to an uncoupled machine. Second, the density of synchrotron resonance lines arising from the presence of sextupoles is also doubled, *although their spacing relative to integer and half integer lines is preserved*. The net result is decreased operating room in the tune plane. There is little that can be done in regards to the “structural” resonances, but the synchrotron resonances driven by dispersion at the sextupoles may be attacked by proper design of a sextupole distribution taking the dispersion into account [4].

A simple two-family sextupole distribution was used for chromaticity correction. In an attempt to minimize the third-order betatron resonance amplitude driven by sextupoles ( $Q_1 = 10.33$ ), a sextupole distribution was designed by traditional methods [5] to minimize the resonance driving terms. Increased operating room was indeed observed in the proximity of the third-order resonance; however there was little effect on the synchrotron resonances.

The region near  $Q_1 = 10.38$  in Figure 3 looks more favorable for operation than the design operating point. Another lattice (C) was designed with operating point  $Q_1 = 9.88$ . The results of a measured tune scan and tracking simulation are shown in Figure 4 for a two-family sextupole distribution. The experimental results show a wider region of stable operation than the previous lattice. A broad region from  $Q_1 = 9.85$  to 9.89 is broken up by a very narrow resonance which is not evident in the tracking results. Furthermore, this quadrant of the tune plane (9.75-10.00) appears to be more favorable from the standpoint of both synchrotron excitation and third-order resonance excitation. In fact, we have verified with a simple model that, in general, the synchrotron amplitudes arising from dispersion in sextupoles are greater in the region  $n < Q_1 < n + 1/2$  than in the region  $n + 1/2 < Q_1 < n + 1$ , although the mechanism for this distinction is not yet understood.

## 4.2 Two-beam Experience

We have also investigated some aspects of two-beam operation. In order to provide beam separation at the north IP, an electrostatic separator bump was constructed using a vertical separator adjacent to the Möbius insert and two horizontal separators on the other side of the insert. Separation at the south IP during injection was provided by powering a single electrostatic separator. We were able to inject both beams to single bunch currents above those in normal HEP operation. We attempted to collide in lattice B but suffered from poor beam lifetimes, presumably due to the single-beam limitations described above. We have not attempted collisions in the other lattices.

## 5 SUMMARY

We have implemented a Möbius insert and designed lattices which allow exploration of the Möbius scheme at CESR. The single-beam dynamics are dominated by the presence

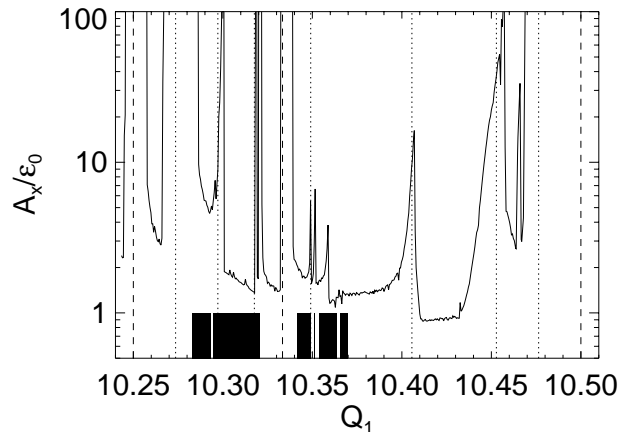


Figure 3: Tune scan results for lattice B. Dashed lines show betatron resonances and dotted lines show synchrotron sidebands. The dark bands are regions with good beam lifetime.

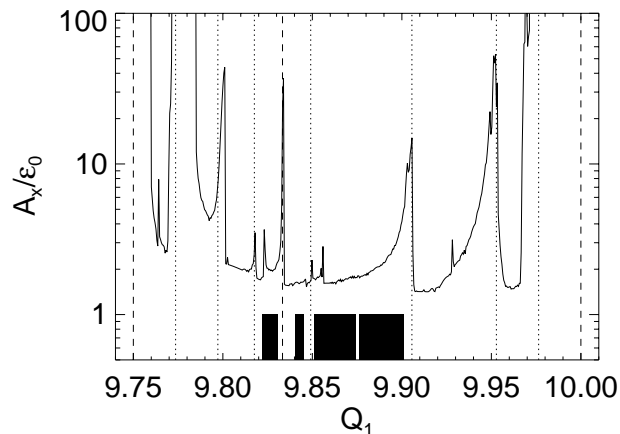


Figure 4: Tune scan results for lattice C.

of strong betatron and synchrotron resonances. The synchrotron resonances are due to dispersion in the chromaticity correcting sextupoles, and are expected to be ameliorated with a design of the sextupole distribution which takes dispersion into account. Despite these features, we observe a favorable operating point near  $Q_1 = 9.88$  and will investigate collisions in this region.

## 6 REFERENCES

- [1] R. Talman, Phys. Rev. Lett. 74 (1995) 1590.
- [2] E. Young et. al., Proc. 1997 Part. Acc. Conf., p. 1542.
- [3] S. Krishnagopal and R. Siemann, Proc. 1989 Part. Acc. Conf. (1989) 836.
- [4] A. Piwinski, Accelerator Physics at the SSC, AIP Conf. Proc. 326 (1995) 202, A. Piwinski, DESY 93-189.
- [5] H. Wiedemann, Particle Accelerator Physics II, Springer-Verlag, 1995, p.146.